Co-assembled photoactive organic molecules into layered double hydroxide as fluorescent fillers for silicone films

Qian Zhang, Yongjun Feng, Rodolphe Valleix, Geneviève Chadeyron, Damien Boyer, Fabrice Leroux

Co-assembled photoactive organic molecules into layered double hydroxide as fluorescent fillers for silicone films

Qian Zhang[a,b], Yongjun Feng[b], Rodolphe Valleix[a], Geneviève Chadeyron[a], Damien Boyer[a*], and Fabrice Leroux[a]

[a]Université Clermont Auvergne, Clermont Auvergne INP, CNRS, ICCF, F-63000 Clermont-Ferrand, France.

[b]State Key Laboratory of Chemical Resource Engineering, Beijing Engineering Center for Hierarchical Catalysts, Beijing University of Chemical Technology, No. 15 Beisanhuan East Road, Beijing 100029, China.

*Corresponding author: Damien Boyer, E-mail: damien.boyer@sigma-clermont.fr

Keywords: Photoactive organic (PAO) molecules; Layered double hydroxides (LDHs); Hybrid materials; Luminescent composite film

Abstract

In this study, photoactive organic molecules (PAO) and polymer stabilizer (anti-oxidant (AO) and light stabilizer (UV)) are co-intercalated into the galleries of layered double hydroxides (LDH) to form a series of new hybrid luminescent LDH fillers, LDH-AO/PAO and LDH-UV/PAO, adjusting the anion ratio of PAO (%). The structure of the hybrid materials is characterized by X-ray diffraction (XRD) and Fourier transform infrared

spectroscopy (FT-IR). The optical properties of the hybrid materials and in particular their absolute photoluminescent quantum yields (PL QY_{ab}) are underlining that the series LDH-(AO or UV)/PAO is excited with varying degrees of efficiency by blue and/or UV-commercial LEDs. Interestingly, it demonstrates that UV and AO hydroxyl-bearing cyclic molecules used here as spacer to disperse PAO molecules are not deleterious to the luminescence. However, less cyclic AO spacer is here preferred to UV light stabilizer to avoid π-π stacking with PAO dyes. An optimal PAO concentration for each composition is determined for the highest PL QY_{ab}. Subsequently, the different samples are dispersed as fillers into silicone to obtain homogeneous luminescent composite films. These results highlight that LDH-(AO or UV)/PAO hybrid materials are suitable candidates to immobilize fluorescent organic dyes and that the associated films are potentially of interest as phosphors materials for several applications.

1. Introduction

Enhancing the luminescence properties of solid-state organic fluorescent materials by inhibiting the aggregation-caused quenching (ACQ) phenomenon while improving their stability for numerous optical applications have always been a key issue.

Photoactive organic (PAO) molecules are attractive for a wide range of applications in coloring, medical treatments, biological labeling, chemical analysis and optoelectronic devices based on light-emitting diodes (LED) **[1-3]**. For instance, fluorescein dye, a well-known PAO molecule, has recently received extensive attention to exploit its unique properties due to its high molar absorbance and excellent quantum yield **[4-6]**. However, as

for the fluorescein, there are some challenges to be solved when facing the applications of photoactive organic molecules for solid-state optical devices: (1) PAO are usually highly sensitive when exposed to moisture, oxygen, heat and light, and its luminescence intensity is quickly quenched **[7]**; (2) most PAO dyes exhibit high luminescence properties when they are highly dispersed in liquid media, while such properties decrease rapidly in solid state by ACQ mechanism **[8]**. Indeed, the dispersion is needed for most PAO molecules in order to maintain suitable optical properties.

To overcome these shortcomings, one approach consists in preventing the aggregation and improving the thermal stability of PAO dyes in solid state. For that purpose, the incorporation of PAO molecules into solid host matrices such as polymers or inorganic materials have been investigated **[9-11]**. Among possible candidates, layered double hydroxides (LDH), $[M^{2+}_{1-x}M^{3+}_{x}(OH)_2](A^{n-}_{x/n}) \cdot mH_2O$, as one kind of anionic clay, have been widely studied to accommodate guest species either by intercalation between their sheets or by adsorption onto their platelets surface **[12-13]**. Because of the noticeable features of LDH, such as adjustable compositions (M^{2+} and M^{3+}) within the host sheet, exchangeable interlayer anions (A^{n-}) in the interlayer region, and tunable charge density (M^{2+}/M^{3+} ratio), the custom design of LDH-PAO hybrid materials is easily performed **[14]**. Additionally, the LDH platelets provide a higher mechanical and thermal stability for the PAO molecules, furthermore they reduce their environmental impact by mitigating their migration. Moreover, LDH platelets are known to be excellent fillers for polymers **[15-16]**. Thus, promising candidate to host PAO molecules in supplying chemical and photochemical stability as well as to prevent their aggregation, LDH host structure is also found to help their implementation

into polymer, which is required to fabricate for example solid-state light-emission or display devices **[17-18]**. It is known that the disaggregation/dispersion of the PAO dyes at the level of the platelets is possible when other molecules are co-intercalated, so literally spacing them from each other. Usually, the spacer used for dilution is a passive molecule, such as a surfactant **[19-21]**. A step further here is to use spacer molecules with peculiar properties which would make the filler multifunctional. To address this issue, a series of large molecules with properties as anti-oxidants and light stabilizers suitable in polymer technology is selected **[22-23]**: 3-(3,5-ditertbutyl-4-hydroxyphenyl) propionic acid (Anti-oxidant (AO), one-fourth of Irganox 1010) and 2-hydroxy-4-methoxy-benzophenone-5-sulphonic acid (UV, UV absorber). The question is here to address if hydroxyl, carbonyl-bearing cyclic organic spacer usually used as light and heat stabilizer is suitable to disperse efficiently dyes molecules when assembled together into the interlayer of LDH host without interacting too much with them to avoid PAO luminescence quenching. PAO dyes with high luminescent quantum yield are Coumarin 343, Coumarin-3-carboxylic acid, Solvent Green 7 and Rhodamine B (abbreviated as C343, C3C, HPTS and RhB, respectively), these dyes are known to accommodate LDH-type host structure **[24]**. All the molecules are presented in **Figure 1**.

In this work, a series of LDH-(AO or UV)/PAO hybrid materials are synthesized through the co-intercalation of photoactive organic molecules and anti-aging molecules. The PAO molecules are introduced into the galleries as a second guest in very small quantities. The presence of anti-aging molecules is expected to prevent the aggregation of PAO molecules as well as to provide them a suitable environment for enhancing their luminescent performances.

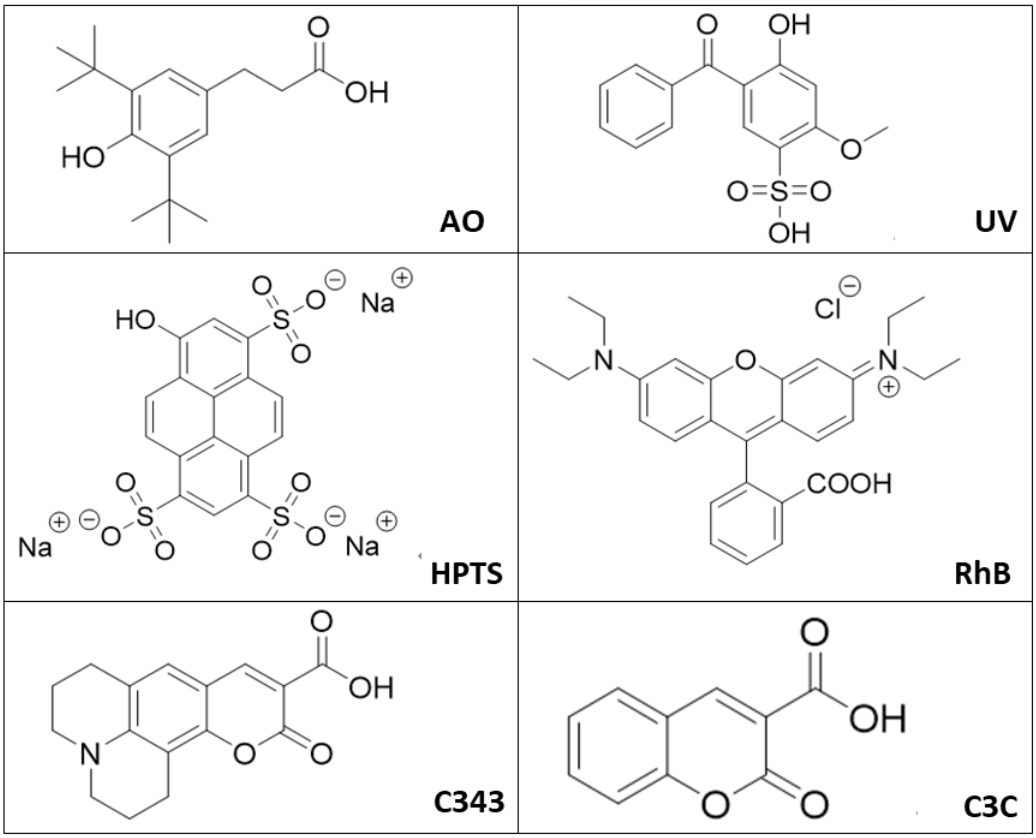

Fig. 1. Organic molecules of AO, UV absorber and PAO.

The chemical composition and the interlayer content of PAO and AO or UV guest anions in LDH-(AO or UV)/PAO are adjusted in the dual compositions: AO/C343, AO/C3C, AO/HPTS, AO/RhB and UV/HPTS. The structural and optical properties of these hybrid LDH-(AO or UV)/PAO materials are investigated by conventional solid-state characterization techniques (XRD and infrared spectroscopy) as well as photoluminescence spectroscopy. Subsequently, luminescent composite films are also achieved by dispersing the LDH-(AO or UV)/PAO fillers into silicone-type polymer matrix. Their optical properties are studied upon blue-UV excitation. These luminescent films could be potentially applied in the fields of luminescent materials for several applications such as display, anti-counterfeiting, or optical design.

2. Experimental section

2.1. Chemicals

All the reagents were of A.R. grade and used as received, such as $Zn(NO_3)_2 \cdot 6H_2O$ (98%), $Al(NO_3)_3 \cdot 9H_2O$ (99%), NaOH (98%), Coumarin 343 (97%), Coumarin-3-carboxylic acid (98%), 8-hydroxypyrene-1,3,6-trisulfonic acid trisodium salt (97%) and Rhodamine B (95%) purchased from Sigma Aldrich. UV absorber 2-hydroxy-4-methoxybenzophenone-5-sulfonic acid (97%) was provided by Alfa Aesar. Antioxidant 3-(3,5-ditertbutyl-4-hydroxyphenyl) propionic acid (AO) was obtained from the hydrolytic reaction of Irganox 1010. The two-component silicone polymer, Bluesil^{TM} RTV 141 part A&B, was supplied by Bluestar Silicones (now Elkem).

2.2. Synthesis of LDH-(AO or UV)/PAO nanofillers

The anti-aging agent and luminescent organic dye co-intercalated LDH-(AO or UV)/PAO were prepared by a one-step co-precipitation method with different concentrations of PAO molecules. Typically, for LDH-AO/C343_n%, 1.74 mmol of $Zn(NO_3)_2 \cdot 6H_2O$ and 0.87 mmol of $Al(NO_3)_3 \cdot 9H_2O$ were dissolved in 50 mL of deionized water to form metal-salt solution. The Zn^{2+}/Al^{3+} solution was added dropwise to 50 mL aqueous solution of AO (a mmol) and C343 (b mmol) containing previously a mmol of NaOH. The value n% stands for the initial molar percentage of C343 in AO and C343 ($n\% = b/(a+b)\times100\%$, $a+b = n(Al^{3+})$). In the addition process, the reactant was vigorously stirred and the pH was kept at 9.5 by using 0.5 M NaOH under nitrogen atmospheric and room temperature conditions. The suspension was aged for another 6 h, then washed three times with deionized water that a clear and

transparent supernatant was obtained. The residual slurry was dried at 40 °C to get the resulting powder for structural analysis and the preparation of Silicone/LDH-(AO or UV)/PAO composite film. In a similar way, LDH-AO/HPTS_n%, LDH-AO/RhB_n%, LDH-AO/C3C_n% and LDH-UV/HPTS_n% were also synthesized. Especially for HPTS intercalated LDH samples: n% = b/(a+b)×100%, a+3b = n(Al^{3+}). The composition of all LDH-(AO or UV)/PAO samples is listed in **Table 1**.

Table 1. The composition of all LDH-(AO or UV)/PAO samples.

LDH samples	Concentration of PAO (%)
LDH-AO/C343	0.01%, 0.05%, 0.1%, 0.5%, 1%, 2%, 3%
LDH-AO/HPTS	1%, 2%, 3%, 5%
LDH-AO/C3C	1%, 2%, 3%, 5%, 10%
LDH-AO/RhB	0.05%, 0.1%, 0.2%, 0.5%, 1%, 2%
LDH-UV/HPTS	0.5%, 1%, 2%, 3%

2.3. Preparation of Silicone/LDH-(AO or UV)/PAO composite films.

The two-component silicone polymer was from two precursors (Bluesil™ RTV 141 A&B): a viscous liquid called part A (90 wt%), which was cured by poly-addition reaction with a catalyst called part B (10 wt%). The LDH-(AO or UV)/PAO powder was used to prepare the silicone/LDH-(AO or UV)/PAO composite film with a loading rate of 40 wt% according to the following process: 2.7 g of part A and 2 g of LDH-(AO or UV)/PAO powder were mixed by a mechanical mixer (Planetary Centrifugal Vacuum Mixer “Thinky Mixer”) at 500 rpm for 10 min, and then pressed in a three rolls mill (Exakt80E) to obtain the homogeneous mixture. The mixture was homogenised again with the mechanical mixer under

the same condition before and after the addition of 0.3 g of part B. Next, the two-component silicone was cast into polymer film onto a Teflon surface (Elcometer 4340 automatic film applicator) at 40 °C with the blade knife height of 200 μm and a casting speed of 30 mm/s. After curing at 80 °C for 2 h, the silicone/LDH-(AO or UV)/PAO composite film was prepared and the film thickness was measured using an Elcometer 456 coating thickness gauge.

2.4. Characterization.

XRD measurements of LDH-(AO or UV)/PAO powders and Silicone/LDH-(AO or UV)/PAO composite films were recorded on a powder X-ray diffractometer (Philips X-Pert Pro) using a Cu Kα source (λ = 0.154 nm). The patterns were collected in a 2θ range from 2.0 to 70.0° with a step size of 1° min^{-1}.

Fourier transform infrared (FT-IR) spectra were performed on a Thermo Scientific Nicolet 6700 FT-IR spectrometer in the range of 4000-400 cm^{-1} with a summation of 32 scans and a resolution of 4 cm^{-1}. Thin KBr pellets were used in transmission mode.

Photoluminescent quantum yields (PL QY) and emission spectra of LDH-(AO or UV)/PAO samples were recorded using a C9920−02G PLQY integrating sphere measurement system from Hamamatsu. The setup includes a 150 W monochromatized Xe lamp, an integrating sphere (Spectralon coating, φ = 3.3 inch) and a high-sensitivity CCD camera. The PL QY_{ab} was defined as the product of the internal photoluminescence quantum yield (PL QY_{int}, i.e. number of emitted photons divided by the number of absorbed photons) by the absorbance (Abs, i.e. the number of absorbed photons divided by the number of exciting

photons). The PL QY_{int} and Abs were given by the C9920−02G PLQY integrating sphere. The relative error on the PL QY_{int} and PL QY_{ab} is ±5%.

The emission spectra of Silicone/LDH-(AO or UV)/PAO composite films were carried out in an integrating sphere with a diode array rapid analyzer system (GL Optic integrating sphere GLS 500) at room temperature. The composite film was placed in a remote phosphor configuration on a blue or UV LEDs emitting at 465, 450 nm and 385 nm respectively, at a distance of 3 mm from the chip. The set of film plus LEDs was then introduced into the integration sphere in order to carry out the measurements.

3. Results and discussion

3.1. Structural analysis of LDH-(AO or UV)/PAO

The XRD patterns of the series of the LDH samples reported in the table 1 with a concentration of PAO of 1% are displayed in **Figure 2**. Four characteristic Bragg reflections of Zn_2Al-LDH are clearly observed, and in each case, they are indexed to the basal reflections (003), (006), (009) and reflection (110) of LDH type structure, thus indicating the formation of layered structure and an intra-layer structural ordering **[25]** respectively, as for all the series. The diffraction reflection (003) at 2θ value of 3.3° and 5.9° corresponds to basal spacing distance of 2.67 and 1.50 nm for LDH-AO and LDH-UV compositions, respectively. Upon the co-intercalation of PAO molecules, the basal spacing remains similar to LDH-AO and LDH-UV, as well as the intensity and width of associated diffraction peaks. The co-assembly of AO/UV and PAO dyes shows no significant effect on the structural coherence length of LDH-(AO or UV)/PAO, as expected from the low relative amount of PAO interleaved

molecules **[26]**. Furthermore, the XRD patterns of the different samples do not indicate the presence of diffraction peaks arising from carbonate phase (expected at 7.6 Å) **[27]**. Hence, the co-precipitation method is efficient for synthetizing co-assembled LDH-(AO or UV)/PAO, and the resulting basal spacing is dominated by the spacer size.

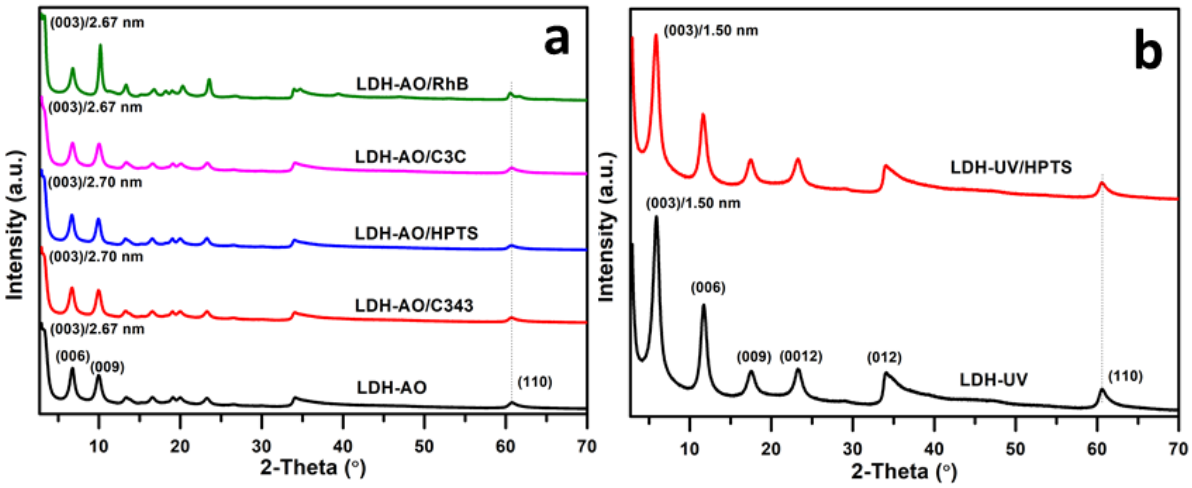

Fig. 2. XRD patterns of (a) LDH-AO/PAO and (b) LDH-UV/PAO.

Figure 3 depicts the FT-IR spectrum of the series LDH-(AO or UV)/PAO with the PAO concentration of 1%. The characteristic IR absorption bands of Zn_2Al-LDH and AO/UV species are observed in all LDH samples: the lattice vibration of M–O and O–M–O (ca. 427 cm^{-1}) from LDH sheets; the broad band O-H stretching vibration (ca. 3435 cm^{-1}) of water and hydroxyl in the brucite-like layer; alkyl group, carbonyl group (ca. 1540 cm^{-1}, 1408 cm^{-1}) and sulfonic group (ca. 1180 cm^{-1}, 1087 cm^{-1}) from AO or UV, respectively **[28]**. Furthermore, the splitting between the asymmetrical and symmetrical mode $\Delta\nu(COO^{-}) = \nu_{as} - \nu_{s}$ evidences the coordination mode between the carboxylate ion and the metal layer of LDH host **[29]**. For LDH-AO/PAO samples, the coordination mode is changed from the monodentate character ($\Delta\nu$ =275 cm^{-1} of AO) to a more chelating character ($\Delta\nu$ = 132 cm^{-1} of LDH-AO/PAO and

LDH-AO). Most probably, since both AO and PAO molecules interact electrostatically with the inner OH-bearing LDH layer surface, there is a change in the symmetry of the carboxylation functional group. In addition, no absorption bands of carbonate or nitrate anions are observed, neither $–CO_3$ (1357 cm^{-1}) nor $–NO_3$ (1383 cm^{-1}), indicating the absence of these two contaminations.

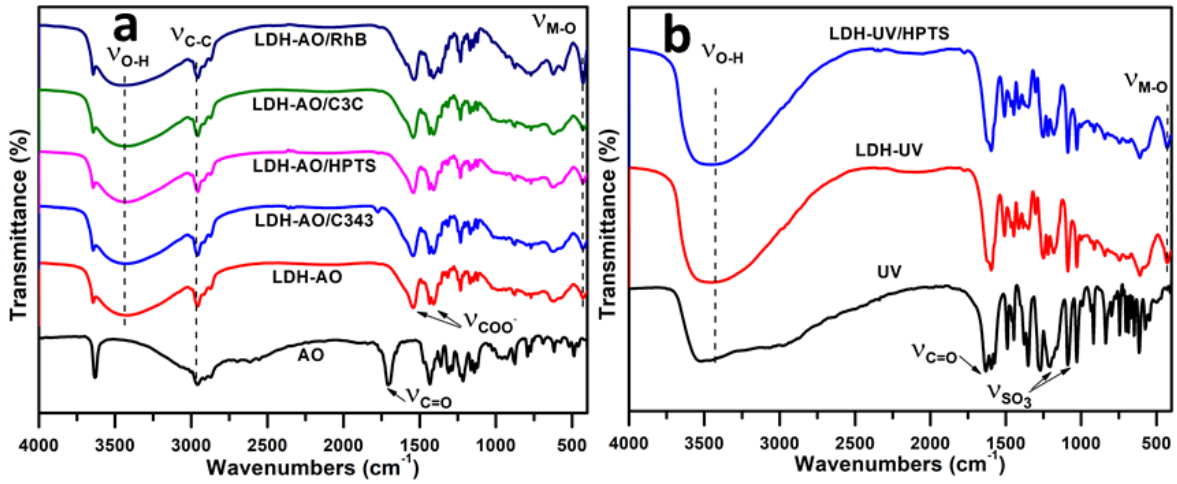

Fig. 3. FT-IR spectra of (a) LDH-AO/PAO and (b) LDH-UV/PAO.

3.2. Photoluminescence properties of LDH-(AO or UV)/PAO

The absolute photoluminescence quantum yields (PL QY_{ab}) as a function of the excitation wavelengths are shown for each sample in **Figure 4**. First of all, it underlines that all the samples are excited more or less efficiently by blue and/or UV-commercial LEDs. For each formulation, an optimal concentration of PAO to give the higher $PLQY_{ab}$ is depicted. For all samples, the PL QY_{ab} drops drastically above a specific concentration that depends on the nature of the PAO.

This observation could be explained by a concentration quenching phenomenon, which is predominant when the concentration of PAO increases above a certain threshold. The same behaviour was pointed out in the case of fluorescein or sulforhodamine B molecules

incorporated into LDH galleries **[21, 30]**. Indeed, when intercalated PAO molecules are sufficiently close to each other in such a restricted space, they are prone to aggregation by π-stacking (parallel stacking) due to conjugated xanthene rings or by hydrogen bonding (head-to-tail). Xanthene dyes **[31, 32]** such as rhodamine or molecules with aromatic rings such as coumarin are well-known to interact mutually, resulting in luminescence quenching when the concentration reaches a critical value to form dimers, trimers, etc.

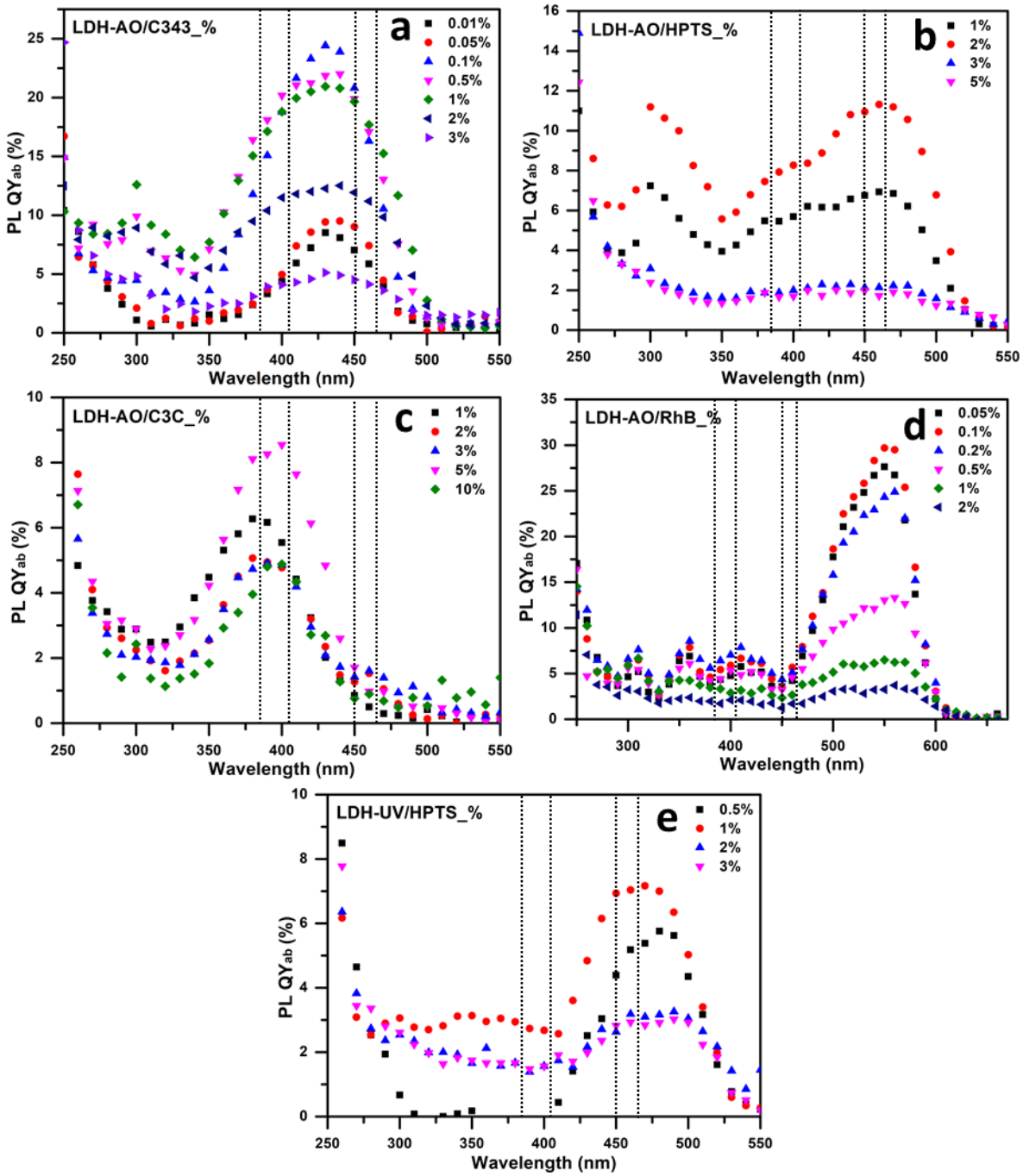

Fig. 4. Variation in PL QY_{ab} of LDH-AO/PAO (a) PAO = C343, (b) PAO = HPTS, (c) PAO = C3C, (d) PAO = RhB and (e) LDH-UV/HPTS. The dotted lines correspond to the excitation wavelength of commercial LEDs.

However, regarding the samples synthesised with the same PAO, i.e. HTPS, but with AO or UV spacers, their PL QY_{ab} profile as function of the wavelength is different. This may be due to their effectiveness, particularly to distribute the luminescent molecules within the interlayer space. In fact, the samples with AO present an extinction by concentration for

doping rates in PAO twice as high as for samples with UV, thus demonstrating the beneficial role of AO on UV spacer to more efficiently disperse the photoactive species in the interlayer space. Compared to AO structure, UV backbone is more suited to interact with its two aromatic rings, which may intensify the π-π stacking effect between close molecules and thus resulting in an aggregate state more pronounced. The sample LDH-AO/HPTS_2% leads to the best absolute PL QY_{ab} with a value of 11% for an excitation at 465 nm, whereas for the same HPTS content, LDH-UV/HPTS sample presents a PL QY_{ab} of 3% only. For the latter, the best photoluminescence quantum efficiency of 7% at 465 nm is recorded for an HPTS concentration of 1%.

Four excitation wavelengths which are of interest since they correspond to UV and blue commercial LEDs (385 nm, 405 nm, 450 and 465 nm) are marked by dotted lines in **Figure 4**. As shown in **Table 2**, we also determined the excitation wavelength leading to the highest PL QY_{ab} which is different for each sample. Regarding the powders LDH-AO/C343 (**Figure 4a**), this matrix can be significantly excited by a UV LED at 405 nm and by a blue commercial LED at 450 nm with PL QY_{abs} of 20% and 20.8%, respectively, for the concentration of 0.1% in C343. For this sample, the maximum PL QY_{ab} (24.4%) of LDH-AO/C343 is reached at λ_{exc} = 430 nm. As the amount of PAO molecules in LDH-AO increases, the PL QY_{ab} is gradually increased up to 0.1% of C343 and then this latter decreases significantly for 3% of C343. As shown in **Figure 4**, a similar behavior occurs for LDH-AO/HPTS (350-550 nm with the maximum PL QY_{ab} at λ_{exc} = 460 nm), LDH-AO/C3C (320-500 nm with the maximum PL QY_{ab} at λ_{exc} = 400 nm), LDH-AO/RhB (450-600 nm with the maximum PL QY_{ab} at λ_{exc} = 550 nm) and LDH-UV/HPTS (400-550 nm

with the maximum PL QY_{ab} at λ_{exc} = 470 nm). It can be noticed that the samples with HPTS, C343 or RhB can be excited, more or less efficiently, either by a UV or a blue commercial LED whereas the hybrid materials with C3C can only be activated by UV LED.

Table 2. The maximum PL QY_{ab} of all LDH-(AO or UV)/PAO samples.

Sample	Concentration of PAO	λ_{exc} (nm)	PL QY_{ab} (%)
LDH-AO/C343	0.01%	430	8.51
	0.05%	440	9.50
	0.1%	430	24.41
	0.5%	440	22.00
	1%	430	20.59
	2%	440	12.51
	3%	430	5.12
LDH-AO/HPTS	1%	460	6.93
	2%	460	11.32
	3%	440	2.29
	5%	430	2.00
LDH-AO/C3C	1%	380	6.27
	2%	380	5.07
	3%	390	4.92
	5%	400	8.55
	10%	400	4.88
LDH-AO/RhB	0.05%	550	27.62
	0.1%	550	29.67
	0.2%	550	24.30
	0.5%	560	13.29
	1%	550	6.50
	2%	560	3.72
LDH-UV/HPTS	0.5%	480	5.76
	1%	470	7.17
	2%	490	3.26
	3%	490	3.02

Considering the potential further association to the emission of a commercial UV/blue LED, the optical properties of the series LDH-(AO or UV)/PAO are investigated upon different excitation wavelengths (385 nm, 450 nm and 465 nm). As shown in **Figure 5**, the emission spectra of LDH-(AO or UV)/PAO with different concentrations of PAO are recorded

at the selected excitation wavelength.

By increasing the ratio of PAO, the fluorescence intensity increases at first and then decreases, and the spectra show a gradual red-shift. Besides, in the case of LDH-AO/C343 (λ_{exc} = 450 nm) and LDH-AO/C3C (λ_{exc} = 385 nm), the emission band covers a wide visible range from 400 to 600 nm with a maximum at about 485 nm (blue). In the case of LDH-AO/HPTS (λ_{exc} = 450 nm) and LDH-UV/HPTS (λ_{exc} = 465 nm), the emission band is between 470 and 650 nm with a maximum at about 525 nm (green). In the case of LDH-AO/RhB (λ_{exc} = 465 nm), the emission band is centred at 600 nm (orange).

The highest PL QY_{ab} values, for each LDH-(AO or UV)/PAO system, recorded at a wavelength of interest, i.e. corresponding to the emission of a commercial LED, are gathered **in Table 3**. Then, the colour coordinates of these five samples with an optimal concentration of PAO molecules (LDH-AO/C343_0.1%, LDH-AO/HPTS_2%, LDH-AO/C3C_5%, LDH-AO/RhB_0.2% and LDH-UV/HPTS_1%) were determined and plotted on a chromaticity diagram (**Figure 6**). It can be noticed that the samples with HPTS, C343 or RhB can be excited, more or less efficiently, either by a UV or a blue commercial LED whereas the hybrid materials with C3C can only be activated by UV LED.

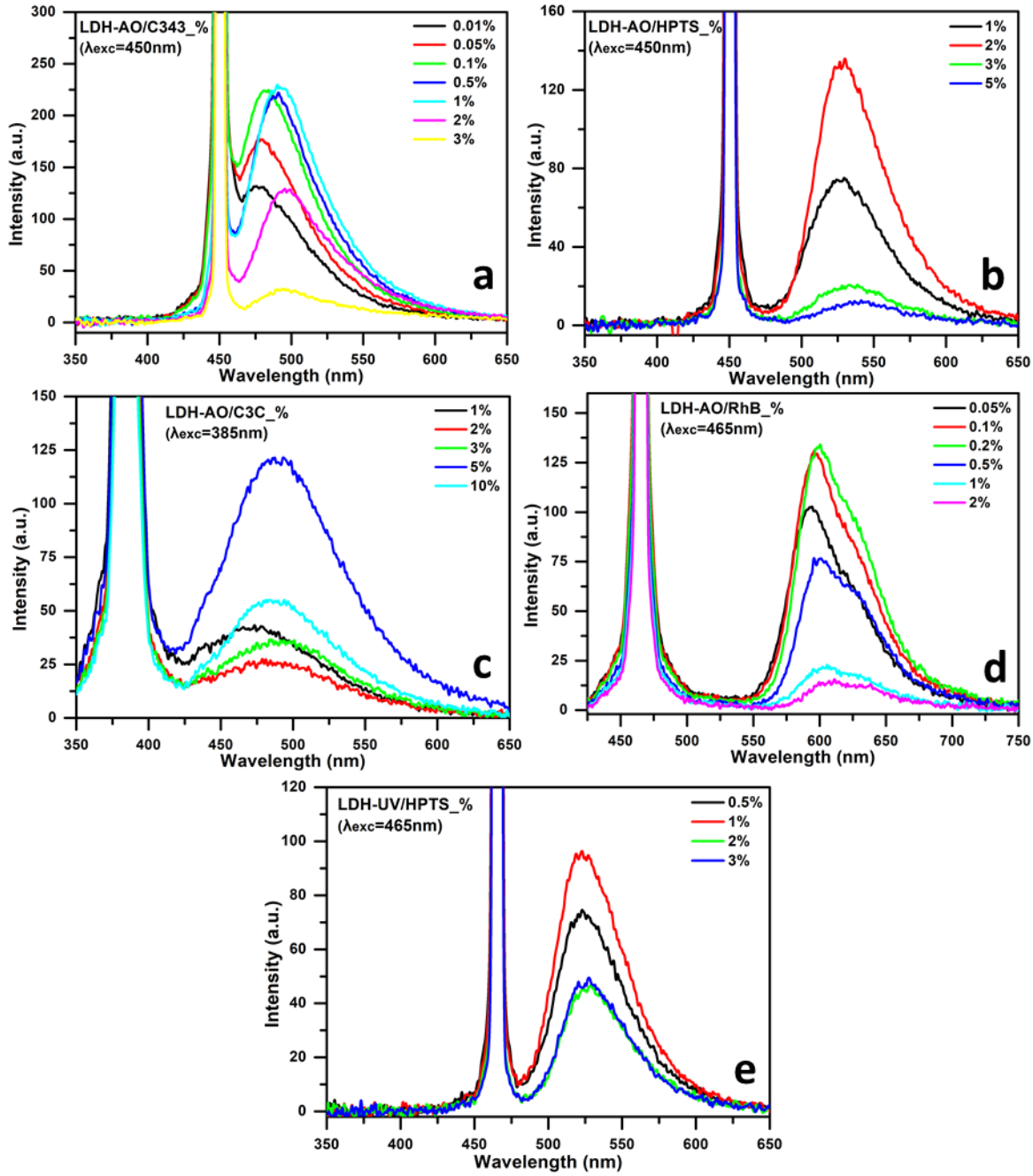

Fig. 5. Emission spectra of (a) LDH-AO/C343 with excitation at 450 nm, (b) LDH-AO/HPTS with excitation at 450 nm, (c) LDH-AO/C3C with excitation at 385 nm, (d) LDH-AO/RhB with excitation at 465 nm and (e) LDH-UV/HPTS with excitation at 465 nm.

Table 3. The highest absolute quantum yield (QY_{ab}) values of powder LDH-(AO or UV)/PAO.

LDH samples	λ_{exc} (nm)	QY_{ab} (%)
LDH-AO/C343_0.1%	450	16.10
LDH-AO/HPTS_2%	450	9.64

LDH-AO/C3C_5%	385	4.50
LDH-AO/RhB_0.2%	465	10.79
LDH-UV/HPTS_1%	465	6.16

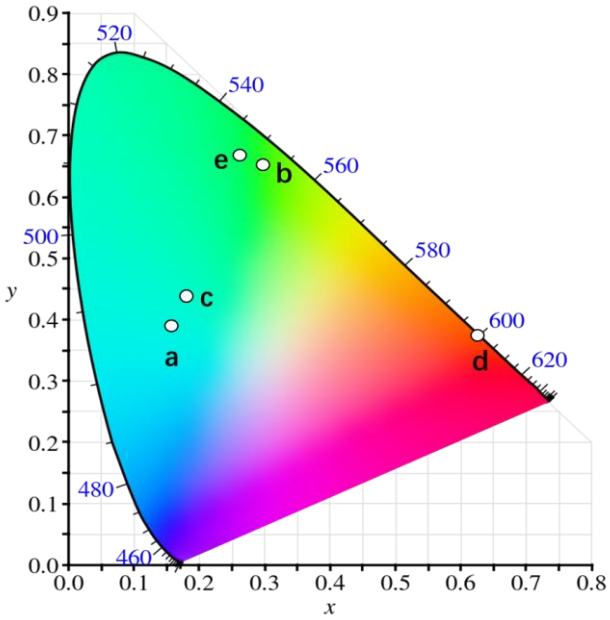

Fig. 6. CIE 1931 chromaticity coordinates for powders of (a) LDH-AO/C343_0.1%, (b) LDH-AO/HPTS_2% measured under 450 nm, (c) LDH-AO/C3C_5% measured under 385 nm, (d) LDH-AO/RhB_0.2% and (e) LDH-UV/HPTS_1% measured under 465 nm.

3.3. Photoluminescence properties of Silicone/LDH-(AO or UV)/PAO composite films.

The silicone composite films loaded with 40% in weight of each LDH-(AO or UV)/PAO sample are processed and exhibit a good transparency indicating that an excellent dispersion of fillers occurs as shown in **Figure 7**.

Fig. 7. Pictures under daylight of the different silicone/LDH-PAO (40 wt%) films: (a) LDH-AO/C343, (b) LDH-AO/HPTS, (c) LDH-AO/C3C, (d) LDH-AO/RhB and (e) LDH-UV/HPTS.

The thickness of the different composite films is measured between 90 and 120 μm.

The emission spectra are recorded upon LED excitation at different wavelengths (465, 450 and 385 nm) as displayed in **Figure 8**.

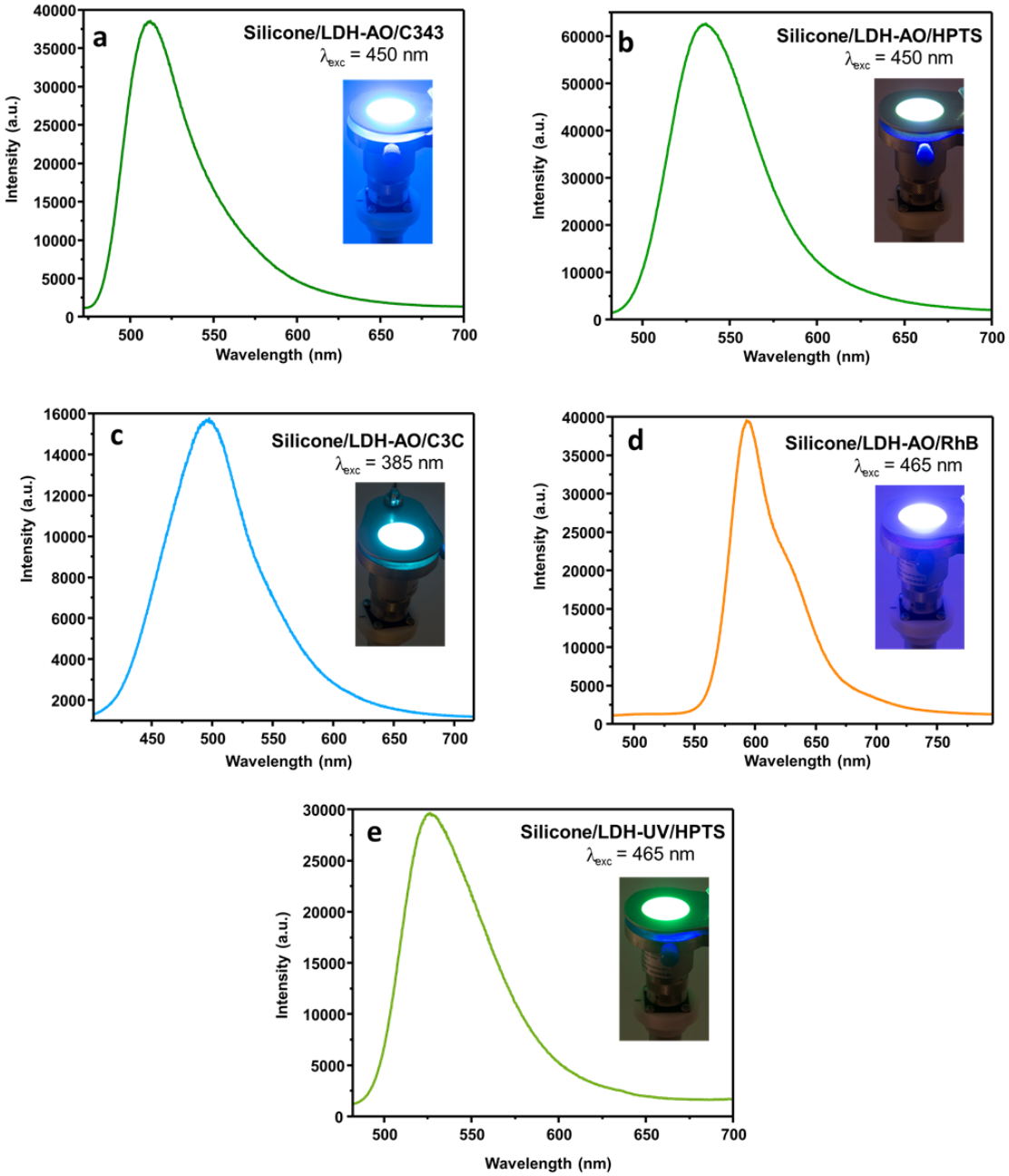

Fig. 8. Emission spectra of the Silicone/LDH-(AO or UV)/PAO composite films measured under LED illumination for (a) LDH-AO/C343, (b) LDH-AO/HPTS, (c) LDH-AO/C3C, (d) LDH-AO/RhB and (e) LDH-UV/HPTS.

One by one, the hybrid luminescent film exhibits a unique profile in terms of maximum peak intensity and shape/broadness of the emission. In the case of AO/C343, the emission band, of high intensity, covers a visible range from 475 to 600 nm with a maximum at 510 nm (green), which is slightly red-shifted compared to that recorded for LDH-AO/C343 powder. This phenomenon can be explained by an aggregation effect of the LDH platelets. The fabrication process of the composite film allows the C343 molecules to aggregate and the distance between molecules is reduced. The green emissions are observed for AO/HPTS and UV/HPTS films (530 nm). In the case of AO/RhB and AO/C3C, the emission band is centered at 490 nm and 590 nm, with the color of blue and orange. To sum up, the dispersion of the LDH-PAO fillers endows the silicone composite with luminescent properties close to optical properties of the pristine hybrid materials.

The chromaticity coordinates were determined for each film and show on the chromaticity diagram in **Figure 9**.

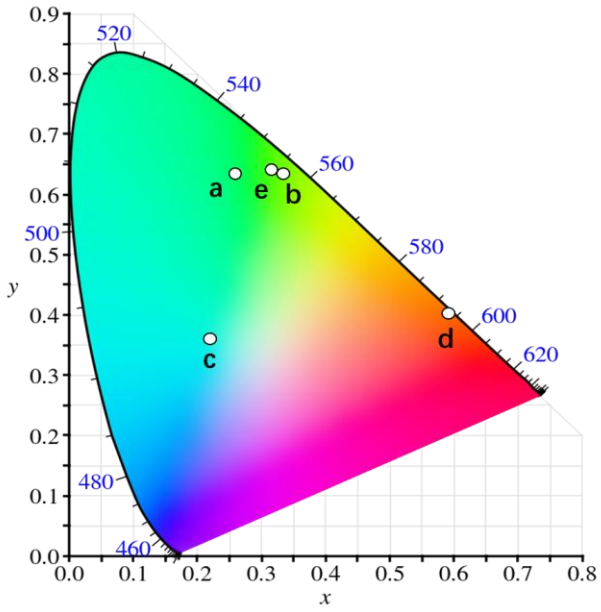

Fig. 9. CIE 1931 chromaticity coordinates of the different silicone/LDH-PAO (40 wt%) films: (a) LDH-AO/C343, (b) LDH-AO/HPTS, (c) LDH-AO/C3C, (d) LDH-AO/RhB and (e) LDH-UV/HPTS.

4. Conclusions

The mixing of co-interleaved photoactive organic molecules (C343, C3C, HPTS and RhB) with anti-aging molecules (AO and UV) into LDH leads to a series of fully characterized hybrid luminescent materials. The AO or UV organic spacer is found to supply a dilution effect for PAO molecules, since the large quantity of AO/UV forces the PAO molecules to be distant from each other, limiting their guest–guest interaction and potential optical quenching. It is also found that AO is preferred here to UV molecules since they interact less with the PAO molecules. Overall, the LDH-(AO or UV)/PAO rank as follows: AO/C343_0.1%, LDH-AO/HPTS_2%, LDH-AO/C3C_5%, LDH-AO/RhB_0.1% and LDH-UV/HPTS_1% powder producing a maximum PL QY_{ab} of 24.4% (λ_{exc} = 430 nm), 11.3% (λ_{exc} = 460 nm), 8.5% (λ_{exc} = 400 nm), 29. 7% (λ_{exc} = 550 nm) and 7.2% (λ_{exc} = 470 nm), respectively. However, under specific UV or blue excitation of interest for LED application, the optimized compositions are slightly changed as AO/C343_0.1%, AO/HPTS_2%, AO/C3C_5%, AO/RhB_0.2% and UV/HPTS_1% to provide suitable blue/green/orange emission. When loaded into silicone, LDH-(AO or UV)/PAO fillers endow the homogeneous composite films with efficient luminescent properties, thus opening new perspectives for further improving LED technology. Further study will be carried out to investigate the stability of these luminescent hybrid materials upon photonic or thermal stresses to assess their ability in operating conditions.

Declaration of competing interest

The authors declare that they have no known competing financial interests or personal

relationships that could have appeared to influence the work reported in this paper.

Acknowledgements

Qian Zhang gratefully acknowledges the National Natural Science Foundation of China (No. U1707603) and the financial support from China Scholarship Council (No. 201906880038).

References

[1] Y. Yang, Q. Zhao, W. Feng, F. Li, Luminescent chemodosimeters for bioimaging, Chem. Rev. 113 (1) (2013) 192–270.

[2] L. Xiao, Z. Chen, B. Qu, J. Luo, S. Kong, Q. Gong, J. Kido, Recent progresses on materials for electrophosphorescent organic light-emitting devices, Adv. Mater. 23 (8) (2011) 926–952.

[3] X. Chen, T. Pradhan, F. Wang, J.S. Kim, J. Yoon, Fluorescent chemosensors based on spiroring-opening of xanthenes and related derivatives, Chem. Rev. 112 (3) (2012) 1910–1956.

[4] K. Rurack, M. Spieles, Fluorescence quantum yields of a series of red and near-infrared dyes emitting at 600-1000 nm, Anal. Chem. 83 (4) (2011) 1232–1242.

[5] J.B. Grimm, B.P. English, J. Chen, J.P. Slaughter, Z. Zhang, A. Revyakin, R. Patel, J.J. Macklin, D. Normanno, R.H. Singer, T. Lionnet, L.D. Lavis, A general method to improve fluorophores for live-cell and single-molecule microscopy, Nat. Methods 12 (2015) 244–250.

[6] L. Yuan, W. Lin, Y. Yang, H. Chen, A unique class of near-infrared functional fluorescent dyes with carboxylic-acid-modulated fluorescence ON/OFF switching: rational design, synthesis, optical properties, theoretical calculations, and applications for fluorescence imaging in living animals, J. Am. Chem. Soc. 134 (2) (2012) 1200–1211.

[7] T.A. Saleh, V.K. Gupta, Functionalization of tungsten oxide into MWCNT and its

application for sunlight-induced degradation of rhodamine B, J. Colloid Interface Sci. 362 (2) (2011) 337–344.

[8] X. Wang, P. Song, L. Peng, A. Tong, Y. Xiang, Aggregation-Induced Emission Luminogen-Embedded Silica Nanoparticles Containing DNA Aptamers for Targeted Cell Imaging, ACS Appl. Mater. Interfaces 8 (1) (2016) 609–616.

[9] R. Boonsin, G. Chadeyron, J.P. Roblin, D. Boyer, R. Mahiou, Silica encapsulated fluorescein as a hybrid dye for blue-LED based lighting devices, J. Mater. Chem. C 4 (27) (2016) 6562–6569.

[10] F.J. Quites, J.C. Germino, T.D.Z. Atvars, Improvement in the emission properties of a luminescent anionic dye intercalated between the lamellae of zinc hydroxide-layered, Colloid. Surface. A 459 (2014) 194–201.

[11] Z. Sun, L. Jin, W. Shi, M. Wei, X. Duan, Preparation of an anion dye intercalated into layered double hydroxides and its controllable luminescence properties, Chem. Eng. J. 161 (1-2) (2010) 293–300.

[12] Q. Wang, D. O'Hare, Recent Advances in the Synthesis and Application of Layered Double Hydroxide (LDH) Nanosheets, Chem. Rev. 112 (7) (2012) 4124–4155.

[13] Z. Gu, J.J. Atherton, Z.P. Xu, Hierarchical layered double hydroxide nanocomposites: structure, synthesis and applications, Chem. Commun. 51 (15) (2015) 3024–3036.

[14] C. Taviot-Guého, V. Prévot, C. Forano, G. Renaudin, C. Mousty, F. Leroux, Tailoring Hybrid Layered Double Hydroxides for the Development of Innovative Applications, Adv. Funct. Mater. 28 (27) (2018) 1703868.

[15] P. Legentil, F. Leroux, S. Therias, R. Mahiou, G. Chadeyron, Revisiting fluorescein and layered double hydroxide using a synergistic approach: A complete optical study, J. Lumin. 215 (2019) 116634.

[16] M. Kotal, A.K. Bhowmick, Polymer nanocomposites from modified clays: Recent advances and challenges, Prog. Polym. Sci. 51 (2015) 127–187.

[17] D. Yan, J. Lu, M. Wei, S. Qin, L. Chen, S. Zhang, D.G. Evans, X. Duan, Heterogeneous Transparent Ultrathin Films with Tunable-Color Luminescence Based on the Assembly of Photoactive Organic Molecules and Layered Double Hydroxides, Adv. Funct. Mater. 21 (13) (2011) 2497–2505.

[18] W. Shi, S. He, M. Wei, D.G. Evans, X. Duan, Optical pH Sensor with Rapid Response Based on a Fluorescein-Intercalated Layered Double Hydroxide, Adv. Funct. Mater. 20 (22) (2010) 3856–3863.

[19] D. Yan, J. Lu, M. Wei, D.G. Evans, X. Duan, Sulforhodamine B Intercalated Layered Double Hydroxide Thin Film with Polarized Photoluminescence, J. Phys. Chem. B 113 (2009) 1381–1388.

[20] D. Yan, J. Lu, J. Ma, M. Wei, S. Qin, L. Chen, D.G. Evans, X. Duan, Thin film of coumarin-3-carboxylate and surfactant co-intercalated layered double hydroxide with polarized photoluminescence: a joint experimental and molecular dynamics study, J. Mater. Chem. 20 (24) (2010) 5016–5024.

[21] P. Legentil, F. Leroux, S. Therias, D. Boyer, G. Chadeyron, Sulforhodamine B-LDH composite as a rare-earth-free red-emitting phosphor for LED lighting, J. Mater. Chem. C 8 (34) (2020) 11906–11915.

[22] Q. Zhang, Y. Guo, A.A. Marek, V. Verney, F. Leroux, P. Tang, D. Li, Y. Feng, Design, fabrication and anti-aging behavior of a multifunctional inorganic-organic hybrid stabilizer derived from co-intercalated layered double hydroxides for polypropylene, Inorg. Chem. Front. 6 (9) (2019) 2539–2549.

[23] R. Ma, T. Chen, Y. Feng, D. Li, Tang. P, Synergetic light stabilizing effects of reducing agent and UV absorber co-intercalated layered double hydroxides for polypropylene, Appl. Clay Sci. 194 (2020) 105700.

[24] J.L. Nyalosaso, R. Boonsin, P. Vialat, D. Boyer, G. Chadeyron, R. Mahiou, F. Leroux, Towards rare-earth-free white light-emitting diode devices based on the combination of dicyanomethylene and pyranine as organic dyes supported on zinc single-layered hydroxide, Beilstein J. Nanotechnol. 10 (2019) 760–770.

[25] Y. Zhao, G. Chen, T. Bian, C. Zhou, G.I. Waterhouse, L.Z. Wu, C.H. Tung, L.J. Smith, D. O'Hare, T. Zhang, Defect-Rich Ultrathin ZnAl-Layered Double Hydroxide Nanosheets for Efficient Photoreduction of CO_2 to CO with Water, Adv. Mater. 27 (47) (2015) 7824–7831.

[26] Q. Wang, X. Zhang, C.J. Wang, J. Zhu, Z. Guo, D. O'Hare, Polypropylene/layered double hydroxide nanocomposites, J. Mater. Chem. A 22 (36) (2012) 19113–19121.

[27] R.M.M. Santos, J. Tronto, V. Briois, C.V. Santilli, Thermal decomposition and recovery properties of ZnAl-CO_3 layered double hydroxide for anionic dye adsorption: insight into the aggregative nucleation and growth mechanism of the LDH memory effect, J. Mater. Chem. A 5 (20) (2017) 9998–10009.

[28] J.T. Kloprogge, D. Wharton, L. Hickey, R.L. Frost, Infrared and Raman study of interlayer anions CO_3^{2-}, NO_3^-, SO_4^{2-} and ClO_4^- in Mg/Al hydrotalcite, Am. Mineral. 87 (5-6) (2002) 623–629.

[29] Q. Zhou, V. Verney, S. Commereuc, I.J. Chin, F. Leroux, Strong interfacial attrition developed by oleate/layered double hydroxide nanoplatelets dispersed into poly(butylene succinate), J. Colloid Interface Sci. 349 (1) (2010) 127–133.

[30] P. Legentil, G. Chadeyron, S. Therias, N. Chopin, D. Sirbu, F. Suzenet, F. Leroux, Luminescent N-heterocycles based molecular backbone interleaved within LDH host structure and dispersed into polymer, Appl. Clay Sci. 189 (2020) 105561.

[31] E. Novoa-Ortega, M. Dubnicka, W.B. Euler, Structure–Property Relationships on the Optical Properties of Rhodamine Thin Films, J. Phys. Chem. C 124 (29) (2020) 16058–16068.

[32] H. Zhang, X. Liu, Y. Gong, T. Yu, Y. Zhao, Synthesis and characterization of SFX-based coumarin derivatives for OLEDs, Dyes Pigments 185 (2021) 108969.